*13th IEA Heat Pump Conference 2020*

**13th IEA Heat Pump Conference**
April 26-29, 2021 Jeju, Korea

# Investigation of model predictive control for fifth generation district heating and cooling (5GDHC) substations

Simone Buffa[a,*], Anton Soppelsa[a], Mauro Pipiciello[a], Gregor P. Henze[b,c], Roberto Fedrizzi[a]

[a] Eurac Research, Institute for Renewable Energy, Viale Druso 1, 39100 Bolzano, Italy
[b] University of Colorado Boulder, Department of Civil, Environmental and Architectural Engineering, Boulder, Colorado 80309 USA
[c] National Renewable Energy Laboratory, Golden, Colorado 80401 USA

**Abstract**

This work investigates the performance of a model predictive controller for customer-sited energy transfer substations, installed in fifth generation district heating and cooling networks (5GDHC) that include electrically driven heat pumps and thermal energy storage systems. Using heat pumps effectively couples the thermal and electrical distribution networks at the individual building level, which opens the door to new scenarios in terms of smart management of urban energy systems. The model predictive controller (MPC) implemented includes two key elements based on artificial intelligence: a composite model of the 5GDHC substation based on several artificial neural networks (ANN) and a constrained optimization solver based on particle swarm optimization (PSO). This study focuses on the analysis performed to test the predictive controller and to understand how it affects the substation energy performance and the building owner's energy bill under different boundary conditions. Moreover, the capacity of the MPC in providing demand flexibility to the power grid has been evaluated through a load shifting strategy obtained by exploiting the capacity of the substation's thermal energy storage.

*Keywords: Smart energy systems; Artificial neural networks; Receding horizon control.*

## 1. Introduction

District heating and cooling is acknowledged as a sustainable solution to meet heating and cooling demands in high-density urban areas. This technology has evolved in the last decades towards low distribution temperature in the network and decentralized active plants and substations. These developments enhance the inclusion of renewable heat sources, a reduction of heat losses with the consequence of a more complicated energy system. Fifth-generation district heating and cooling (5GDHC) systems operate at a temperature range between 0÷30°C that is not suitable for direct heating purposes even with low-temperature heat emission systems like floor heating or ceiling panels. Because of the neutral temperature of the network with respect to the ground, heat losses are minimized, and all available urban low-temperature excess heat can be recovered and reused according to circular economy principles. These pros are paid for with the fact that water-source heat pumps, usually electrically driven, are needed in the customer-sited energy transfer stations to boost the temperature of the supplied heat to satisfy the user comfort as shown in Fig. 1. 5GDHC substations can be hydraulically complicated compared to traditional district heating (DH) user substation and in general, are operated to supply space heating (SH) and domestic hot water (DHW) or active/passive space cooling (SC). Consequently, a reversible 5GDHC substation can be considered a "prosumer" that can extract heat from the thermal network in heating mode as a common end-user, or that can supply heat to the network in cooling mode as a producer.

The interest in 5GDHC systems is growing in Europe with an installation rate of three systems per year on average in the last decade [1]. Existing 5GDHC networks will be expanded and new ones will be built in the

* Corresponding author. Tel.: +39-0471-055636; fax: +39 0471 055 699
*E-mail address:* simone.buffa@eurac.edu

framework of the Interreg project D2grid [2] and H2020 REWARDHeat [3], both launched in 2019. Several utility companies have started exploiting the advantages of supplying simultaneously heating and cooling by means of a single network, extending the operation of the DHC system and their economic revenues all year round.

This study focuses on the development of an advanced decentralized controller for 5GDHC substations with a focus on the optimization of DHW production. The method adopted for the controller implementation is presented in Section 2 whereas the results of preliminary tests are discussed in Section 3.

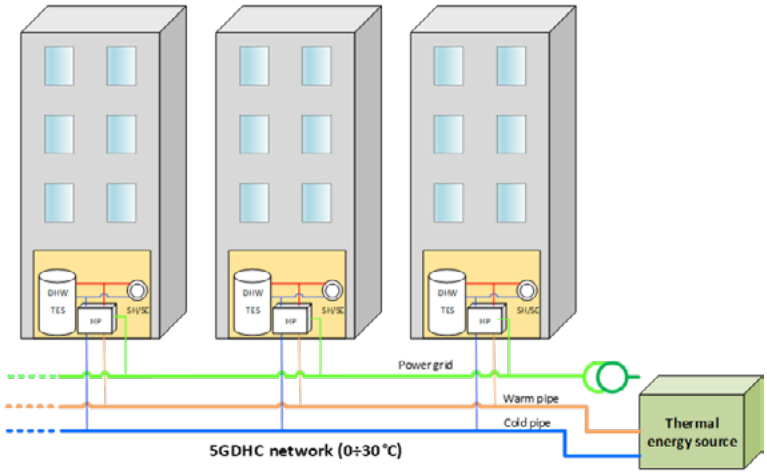


Fig. 1. Layout of a 5GDHC system.

## 2. Methodology

The advanced controller for 5GDHC substations has been implemented in the form of artificial neural network-based model predictive control (ANN-MPC). A literature review about the MPC application for HVAC systems can be found in Afram and Janabi-Sharifi (2014) [4].

In general, MPC employs an explicit model of the system whose identification phase is usually demanding in terms of development time and effort. At each control timestep, the state of this model is updated from measurements, and the model is used to make several predictions of the future behaviour of the system according to a sequence of the control inputs $\bar{u}(t)$ that are applied. MPC is a form of optimal control since it involves an optimization algorithm that solves in real-time a constrained optimization problem providing the sequence of the control variables that minimises (or maximises) a given objective function over a time window, satisfying the problem constraints. At the current time-step $t$, only the first value of the optimal trajectory identified by the MPC is applied to the system. At the next control timestep $t+1$, the procedure is repeated with a prediction horizon window shifted by one control timestep. This methodology is known as receding horizon model predictive control approach. To limit the computational effort of the controller, it is a common practice to apply a move blocking strategy so that the length $M$ of the control input vector $\bar{u}(t)$ is shorter than the prediction horizon length $N$ and the last element of control input vector $\bar{u}(t)$ is kept constant for the remaining timestep of the prediction horizon.

MPC can be applied in general in the form of a multi-input multi-output (MIMO) system that aims at minimising an objective function that includes a tracking error with respect to a reference value and the control effort over the prediction horizon. Conversely, as in this study, MPC can be also employed as a supervisory controller developed in the form of an economic MPC since the objective function to be minimised includes system economics. A black-box model of the considered system has been developed in the form of artificial neural networks (ANNs). This reduced-order model (ROM), presented in the next section, has been used as a surrogate model of the real system to perform at each control timestep $t$ a prediction of its performance over the prediction horizon.

*2.1. Reduced order model (ROM) of the 5GDHC substation*

Reduced order models (ROMs) is the term used for simplified models of complex systems that can capture the system performance maintaining adequate accuracy. The growing application of machine learning algorithms in building energy systems allow the development of ROMs that in general exhibit the following advantages (+) and disadvantages (-) with respect to fully defined physics-based building energy models:

(+) the building and the energy system feature do not need to be fully defined;
(+) simplified models can be aggregated to build complex models with a bottom-up approach;
(+) they have a short simulation runtime that is important especially in real-time systems;
(+) a predefined model architecture can be employed in different case studies;
(-) to create the model a diverse training dataset is needed so that the model can experience different possible conditions;
(-) the model outputs depend on the temporal resolution of the training dataset;
(-) the model outputs cannot be explained by physical laws and must be interpreted.

There are several ways to build data-driven ROMs of HVAC systems. In particular, in Afram and Janabi-Sharifi (2015) [5] artificial neural networks (ANNs) outperform different black-box models as well as grey-box models of the same HVAC components installed in a single-family house. Moreover, in Esen and Inalli (2010) [6], [7] and in Li et al. (2011) [8] it was shown that adaptive network-based fuzzy inference system (ANFIS) models overperform ANN models for a ground-source heat pump (GSHP) system and for the prediction of the building electricity, hot and cold water loads, respectively. Nevertheless, ANFIS models require more complicated architectures as well as more complicated training algorithms. For this reason, the present study focuses on the development of ROMs based on ANNs that can be used in a real-time control system for a 5GDHC substation.

ANN-based MPC consists of the application where a single ANN model or a group of interconnected ANN models are used as a surrogate model of the system in an MPC controller [9]. Afram et al. (2017) [10] performed an extensive review of the application of ANN-MPC for the optimization of HVAC systems operation. The authors highlighted that this approach has been applied especially in commercial, public and office buildings in the last years because the HVAC systems of such large buildings are usually equipped with a building energy management system that can handle the outputs of an MPC controller. This is not the case for residential buildings that represent the largest share of the building stock. Nevertheless, residential buildings can harness several economic and environmental advantages through the exploitation of MPC technology and can provide flexibility to both electrical and thermal grids. Since 5GDHC systems pave the way for decentralised sector coupling exploiting customer-sited energy transfer substations, the ANN-MPC technology has been developed to operate a substation of this kind supplying a small multifamily house.

*2.2. Optimization algorithm*

As is described in Afram et al. (2017) [10], different nonlinear optimization methods have been used in the field of ANN-MPC like genetic algorithms (GA), Newton-Raphson, branch and bound, etc. Nevertheless, among the metaheuristic methods, GA is the most widely used in ANN-MPC studies. It is able to solve both constrained and unconstrained problems and to deal with integer values. These pros are paid for with slow convergence for complex problems so that it can be not suitable for real-time implementation. Particle swarm optimization (PSO) algorithm is considered a well-balanced method to solve both single and multi-objective optimization problems with low computational time [10]. For this reason, this optimization algorithm has been chosen in this study for the implementation of a real-time MPC controller.

PSO is a biologically inspired meta-heuristic methodology. This population-based algorithm is useful in solving optimization problems where the analytical expression of the gradient of the cost function is not available or difficult to assess. It consists of a population of interacting agents that directly search for the minimum of the cost function in a multi-dimensional domain with no information about the gradient (unknown environment). It is inspired by the collective behaviour of species like birds (flocking) and fishes (shoaling and schooling). This concept is part of the artificial intelligence discipline under the name of “swarm intelligence”. The LabVIEW code used in this work was derived from the “perturbed Particle Swarm Optimization” (pPSO) algorithm that is part of the Advanced Metaheuristics Algorithms library implemented by Derouiche M. L. (2015) [11] on the basis of the work of Xinchao Z. (2010) [12], and available at [13].

The algorithm implemented by Derouiche M. L. (2015) has been designed to have as output a real number. Nevertheless, since the HP of the 5GDHC substation operates in ON-OFF mode the algorithm has been modified to handle a binary output. This has been done according to the proposal of Kennedy and Eberhart (1997) [14] where the velocities of the particles are treated as "probabilities of change" and their position results in a 0 or 1 state.

### *2.3. Physical model of a 5GDHC substation*

In order to build the reduced order model (ROM) of the 5GDHC substation, a physical model in TRNSYS [15] has been set up in order to create a dataset used for training the data-driven model based on artificial neural networks (ANNs). The physical model of the 5GDHC substation has been built using Type 927 of the TESS library to model the water-source heat pump (WSHP) system and Type 534 of the TESS library to model the DHW TES and the SH/SC buffer tanks. The 5GDHC network is not modelled and it is considered an ideal thermal energy source that supplies the substation at a constant temperature of 15°C. The 5GDHC substation has been sized to meet the space heating (SH) and domestic hot water (DHW) demands of a small multi-family house located in Rome and has a thermal capacity of about 23 kWth. The residential building has a total of 10 apartments divided into 5 floors. Every single apartment has a floor area of 50 m2 and an energy net demand level of about 45 kWh/m2 per year for space heating (SH) according to the study performed in Fedrizzi et al. (2015) [16]. Accordingly, the specific DHW load results in 24 kWh/m2 per year and it has been obtained by generating the DHW draw profile by means of the tool DHWcalc V.2.02b [17] considering an occupancy level of 2 people/apartment and specific hot water demand of 40 l/(person day). The building heat emission system consists of ceiling radiant panels that are supplied by the 5GDHC substation. The SH demand profile has been obtained from a separate dynamic numerical simulation of the building using Type 56 and used as a boundary condition for the substation.

The performance map of the water source heat pump (WSHP) has been calibrated and validated by means of dedicated tests at the Energy Exchange Laboratory of EURAC Research in Bolzano-Bozen (Italy) [18]. The tests have been performed by first fixing a constant inlet temperature at the evaporator and varying the inlet temperature at the condenser, thereafter fixing a constant inlet temperature at the condenser and varying the inlet temperature at the evaporator. The results of the calibrated HP model concerning the thermal power measured at the evaporator and condenser as well as the electricity consumption fall within the measurement uncertainty band under almost all operating conditions.

### *2.4. Reduced order model (ROM) of a 5GDHC substation*

The reduced order model (ROM) of the 5GDHC substation has been built by adopting a modular approach and using one ANN to model each single component. The composite model of the 5GDHC substation is obtained by connecting, in a proper way the input-output of an ANN model of the DHW TES system and an ANN model of the HP. To achieve this goal, the two ANN models have been trained separately using a dataset of 20 days obtained from the TRNSYS simulation of the validated 5GDHC substation model. The time resolution adopted to model the system is 10 minutes, short enough to capture the system dynamics and allowing the possibility of taking into account a "cost" for the change of state (ON-OFF) of the HP. This timestep is also large enough to keep the computational effort acceptable. The same control timestep of 10 minutes has been adopted for the optimization problem of the MPC. It is important that the ANN models are developed with the same timestep of the optimization problem so that during the MPC real-time simulation the variables exchanged, that are in this case thermal energy, are the results of the integration of thermal power profiles over the same control timestep. The ANN structure adopted in this study for the two models is the same: nonlinear autoregressive network with exogenous inputs (NARX). This kind of ANN differs from the standard multilayer perceptron (MLP) because includes feedback from the outputs.

The variables considered in the development of a 5GDHC substation ANN model are listed in Table 1. The thermal energy delivered by the HP to the DHW TES ($E_{th,HP,DHW}$) in one control timestep (4 kWhth) represents the control variable and its trajectory is provided according to the binary output of the MPC. During the MPC simulation, the trajectories of $E_{th,HP,DHW}$ are provided to the ANN model to perform an on-line simulation. This variable is provided to both the TES and HP models, simultaneously. The DHW TES system ANN model inputs are the thermal energy supplied to the DHW TES by the HP ($E_{th,HP,DHW}$) and the DHW load covered by the DHW TES ($E_{th,load}$). The two outputs are the temperature at the top ($T_{top}$) and at the bottom ($T_{bot}$), respectively. The ANN has 15 neurons in the hidden layer where the tangent-sigmoid activation function has been used, whereas for the output layer the linear activation function has been adopted.

The ANN model of the HP has 15 neurons in the hidden layer. The tangent-sigmoid and the linear activation functions have been adopted in the hidden and output layer, respectively. The model inputs are three: the thermal energy provided by the HP to the DHW TES ($E_{th,HP,DHW}$), the inlet temperature of the HP at the condenser ($T_{in,load}$) and the inlet temperature of the HP at the evaporator ($T_{in,source}$). The model provides as outputs the electricity consumption of the substation ($E_{el,SUB}$) and the thermal energy extracted by the HP from the DHC network ($E_{th,SUB}$).

Table 1 Inputs and outputs description of the implemented ANN models.

| | | **ANN Model of the TES** | | **ANN Model of the HP** | |
|---|---|---|---|---|---|
| | | Input variables | Output variables | Input variables | Output variables |
| Input at | $t = t_k$ | 1- $E_{th,HP,DHW}$ $[kWh]$<br>2- $E_{th,load}$ $[kWh]$ | 1- $T_{top}$ $[°C]$<br>2- $T_{bot}$ $[°C]$ | 1- $E_{th,HP,DHW}$ $[kWh]$<br>2- $T_{in,load}$ $[°C]$<br>3- $T_{in,source}$ $[°C]$ | 1- $E_{el,SUB}$ $[kWh]$<br>2- $E_{th,SUB}$ $[kWh]$ |
| Input TDL at | $t = t_{k-1}$ | 3- $E_{th,HP,DHW}$ $[kWh]$<br>4- $E_{th,load}$ $[kWh]$ | | 4- $E_{th,HP,DHW}$ $[kWh]$<br>5- $T_{in,load}$ $[°C]$<br>6- $T_{in,source}$ $[°C]$ | |
| Output TDL at | $t = t_{k-1}$ | 5- $T_{top}$ $[°C]$<br>6- $T_{bot}$ $[°C]$ | | 7- $E_{el,SUB}$ $[kWh]$<br>8- $E_{th,SUB}$ $[kWh]$ | |

The validation of the ANN models has been performed comparing the outputs with a dataset from a physical model simulation of 24 hours (144 timesteps of 10 minutes) not used for the ANN training. The performance metrics assessed for this purpose over the entire simulation are the normalised mean bias error and the coefficient of variation of the root mean square error for the variable $\zeta_j$ presented in Equations 1 and 2, where $m_i$ the measured value and $s_i$ is the simulated one of the variable $\zeta_j$.

$$NMBE_{\zeta_j} = \frac{1}{\bar{m}_j} \frac{\sum_{i=1}^{n}(m_{j,i} - s_{j,i})}{n} \cdot 100(\%) \quad (1)$$

$$CVRMSE_{\zeta_j} = \frac{1}{\bar{m}_j} \sqrt{\frac{\sum_{i=1}^{n}(m_{j,i} - s_{j,i})^2}{n-1}} \cdot 100(\%) \quad (2)$$

For the ANN model of the DHW TES a CVRMSE of 2.1% has been obtained for the temperature at the top ($T_{top}$) and a CVRMSE of 4.9% for the temperature at the bottom ($T_{bot}$). For the ANN model of the HP a CVRMSE of 1.3% has been achieved for the electricity consumption ($E_{el,SUB}$) and a CVRMSE of 0.8% has been achieved for the thermal energy extracted by the HP from the source ($E_{th,SUB}$). The NMBE for all the variables resulted in less than 1%.

### *2.5. Cost function*

The MPC controller has been implemented as an economic MPC task since the objective function to minimise is the operating costs of the 5GDHC substation over the prediction horizon with $N$ timesteps $[t_0, \dots, t_k, \dots, t_{k+N-1}]$. As shown by Equation 3 the operating cost calculation considers at each timestep $t_j$, $E_{el,SUB}(t_j)$: the electricity consumption of the substation and its auxiliaries, $c_{el}(t_j)$: the specific cost of electricity, $E_{th,SUB}(t_j)$: the thermal energy supplied by the 5GDHC network to the substation and $c_{th,dhc}(t_j)$: its specific cost.

$$J(t_j) = \sum_{j=k}^{k+N-1} c_{el}(t_j) E_{el,SUB}(t_j) + \sum_{j=k}^{k+N-1} c_{th,dhc}(t_j)\, E_{th,SUB}(t_j) \quad (3)$$

Moreover, in order to minimise the number of ON-OFF switching events of the HP that are cause of inefficiencies and stress for both electrical and mechanical components as shown by Curtis and Pine (2012) [19], a "state change cost" $K(t_j)$ has been added in the cost function and implemented according to Equation 4: the state variations of the HP over the prediction horizon $N$ are counted and weighted by a factor $\beta$ that has been set equal to 1 in this study.

$$K(t_j) = \beta \sum_{j=k}^{k+N-1} \left| s(t_j) - s(t_{j-1}) \right| \quad (4)$$

The PSO algorithm used here has been conceived to solve unconstrained problems. To handle the MPC problem, the constraints have been included in the cost function in the form of soft constraints as suggested by Derouiche et al. (2016) [11]. The method applied here is the external static penalty technique so that the value of the objective function increases proportionally to the degree of constraint infeasibility. The constrains must be verified over the control horizon and are implemented as follows:

- the temperature at the top of the DHW TES must be higher than 45°C to satisfy the comfort needs as described by Equation 5:

$$\min_{t_j \geq 0} T_{top,DHW}(t_j) > T_{top,DHW,min} = 45°C \quad (5)$$

- the temperature at the top of the DHW TES must be lower than 55°C to satisfy the operating limits of high temperature and high pressure of the refrigerant at the HP condenser that has been verified through dedicated tests at the Energy Exchange Laboratory:

$$\max_{t_j \geq 0} T_{top,DHW}(t_j) < T_{top,DHW,max} = 55°C \quad (6)$$

The overall cost function is implemented so that at each control timestep it is called by the optimization algorithm and it is assessed considering the different trajectories of the ANN model outputs and of the boundary conditions over the prediction horizon $N$. To increase the robustness of the controller, the MPC outputs are filtered through a back-up rule-based controller (RBC) so that the DHW TES is charged if the temperature at the top accidentally drops below 45°C or it is no longer charged if the temperature at the top could reach a value higher than 55°C.

In the next section, the results of two separated tests are presented with a perfect prediction of the DHW load. In both cases, a prediction horizon of three hours $(N = 18)$ and a control horizon of one hour $(M = 6)$ have been selected. Test 1 deals with the assessment of the behaviour of the MPC controller both with and without model mismatch between the model used in the MPC and the one used to simulate the controlled system. In Test 2 the results of different scenarios over a simulation of one month (January 2017) are presented. The boundary conditions include a time-of-use (TOU) electricity price variation as a form of demand response (DR) strategy based on the Italian tariff D1 taken as a reference. According to this, the peak period is defined as the time between 8:00 and 19:00 on work days. The aim is to compare the results of a standard rule-based control (RBC) strategy versus MPC only to cover the DHW load through the assessment of the following KPIs:

- $T_{top,max}$ and $T_{top,min}$ are the maximum and minimum temperature value at the top of the DHW TES (controlled variable) over the simulation period;
- $T_{ave}$ is the volume average temperature the DHW TES over the simulation period;
- $E_{el,sub}$ and $E_{th,sub}$ are the electricity and thermal energy consumptions of the substation coming from the electrical and thermal grids during the DHW operation mode;
- $E_{load}$ is the DHW load covered by the substation;
- $COP_{sub}$ is the coefficient of performance of the substation including the HP and auxiliaries in DHW operation mode calculated as the ratio between $E_{load}$ and $E_{el,sub}$;
- $N_{on}$ is the total number of the HP start-ups in DHW operation mode;
- $E_{el,sub,off\text{-}peak}$ and $E_{el,sub,peak}$ are the electricity use of the substation during the off-peak and peak hours;
- $t_{disc}$ is the percentage of time with respect to the entire simulation period where the DHW is available for the user at a temperature lower than 44°C. This limit has been fixed as a threshold to assess a form of discomfort for the final user.

The simulations of Test 2 are performed in TRNSYS and have a time step of one minute that allows observing with enough resolution the interaction between the HP and the DHW TES that influence the TES stratification process. The controller that includes the MPC and the backup controller is implemented in LabVIEW. The MPC optimization problem is solved with a control timestep of 10 minutes. To exchange information between TRNSYS and LabVIEW in real-time a dynamic link library (DLL) connection has been developed.

## 3. Results and discussion

### *3.1. Test 1: No model mismatch vs. model mismatch*

The first test involving the MPC controller aims at comparing its operation through the two platforms developed for the debugging phase: the first one realised completely in LabVIEW and the second one includes a co-simulation between TRNSYS and LabVIEW. A model to emulate the real system is needed in the debugging phase to test the ANN-MPC. In both cases, the emulator is updated at each control timestep by receiving the first input u* of the optimal trajectory resulting from the MPC calculations and returns back state information about the "virtual system" to update the state of the MPC model before the optimization process starts again. In the first platform, the same ANN model of the MPC controller is used as an emulator of the 5GDHC substation (no model mismatch) whereas in the TRNSYS platform a physical model of the substation is used for the same purpose with the introduction of a mismatch between the MPC model and the system emulator.

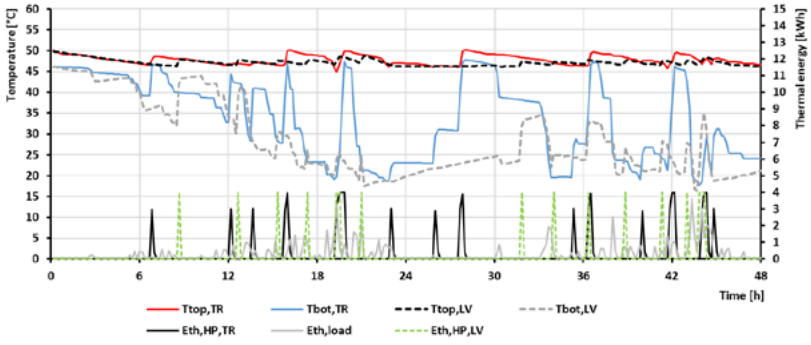


Fig. 2. Simulation results of the "no model mismatch" case VS the target values.

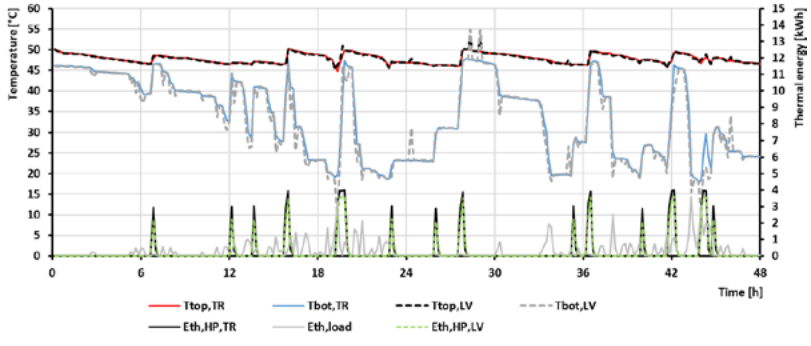


Fig. 3. Simulation results of the "model mismatch" case VS the target values.

In Fig. 2 the simulation results of the two cases with model mismatch (TRNSYS platform) and without model mismatch (LabVIEW platform) are compared under the same boundary conditions for testing the MPC during a simulation duration of 48 hours: the DHW TES model starts with the same state-of-charge in the two

simulations and the identical DHW load is applied. On the primary axis, there are shown the temperature profiles at the top and at the bottom of the DHW TES. The solid lines Ttop,TR, Tbot,TR represent the target temperature profiles that are the result of the physical model of the substation developed in TRNSYS. The dashed lines Ttop,LV, Tbot,LV represent the temperature profiles of the ANN model of the substation developed in LabVIEW. On the secondary axis, there are shown the thermal energies supplied by the HP to the DHW TES in the two cases (Eth,HP,TR, Eth,HP,LV) and the DHW load considered (Eth,load) with a timestep of 10 minutes. It can be noticed that after a few hours of simulation the temperature profiles of the ANN model in LabVIEW (no model mismatch case) diverge from the true profiles that one obtains from the TRNSYS model (model mismatch case). A normalised error for the temperature at the top ($CVRMSE_{Ttop,LV}$) of 3% and for the bottom one ($CVRMSE_{Tbot,LV}$) of 28% for the entire simulation is observed. These results are a consequence of the use of NARX ANNs models that propagate the errors for the output variables at the current timestep to the model inputs at the next timestep.

In Fig. 3 the same profiles of the previous case are shown, but the comparison is made between the outputs of the TRNSYS model and the real-time outputs of the surrogate ANN model of the MPC (model mismatch case). It can be noticed that since at each control timestep the ANN model state is initialised from the true measurements of the system (output of the TRNSYS model) the error that it provides to the outputs is very small and is not propagated along the simulation. This small error is also due to the delay of one simulation timestep (1 minute) that occurs during the exchange of information between the TRNSYS-LabVIEW co-simulation process. The errors of the temperature profiles are reduced to a value of 0.7% for $CVRMSE_{Ttop,LV}$ and a value of 6.3% for $CVRMSE_{Tbot,LV}$. Beyond this comparison, it can be observed that the MPC satisfies the constraints of the top temperature of the TES described by Equation 5.

### *3.2. Test 2: rule-based control vs. model predictive control*

The test of the MPC controlled described in this study aims at comparing its performance with respect to a baseline that represents a simulation with the same boundary conditions where the 5GDHC substation is operated by a rule-based control strategy. Three scenarios have been developed to test the MPC operation and to perform an energetic and economic performance assessment of the 5GDHC substation for supplying the DHW load. The difference between the three MPC scenarios is the profile of the electricity price. It is flat and equal to 0.15 [EUR/kWh] for the scenario 1, whereas it is 0.15 [EUR/kWh] during the off-peak hours and equal to 0.30 [EUR/kWh] and 0.60 [EUR/kWh] during the peak-hours for the TOU scenario 2 and 3, respectively. The price of the thermal energy extracted from the 5GDHC grid has been considered constant and equal to 0.05 [EUR/kWh]. Thus, a TOU-based demand response is implemented only in scenarios 2 and 3 since in scenario 1 the electricity price is constant and the MPC operates to minimise the energy consumptions and state change of the substation.

The results listed in Table 2 show that in scenarios 1, 2 and 3 the MPC operates by charging the DHW TES more frequently with respect to the baseline scenario. In fact, the number of start-up signal (Non) of the HP in DHW mode increases by about 70.3%, 57.4%, and 67.3%, respectively. Thus, on average it results that less thermal energy is provided by the HP to the DHW TES during a single charge with respect to a standard charging process that occurs in the baseline scenario. The same occurs for the average electricity extracted by the HP from the power grid in a single charging process. The MPC always operates to further increase the temperature of the TES when a peak in the load is predicted. This occurs also in scenario 1 where the electricity price is flat. Nevertheless, the temperature at the top of the TES never reaches the upper bound of 55°C. The extra-charging process of the MPC has an impact on the average temperature of the TES over the simulation period that increases between 1.4% and 1.9% for the different scenarios with respect to the baseline with resultant higher thermal losses of the TES but achieving a reduction of the discomfort period (tdisc) for the occupant. Since the temperature at the evaporator is maintained constant, a higher temperature at the condenser has a negative impact on the COPsub that drops by about 3÷3.7% in the different scenarios with respect to the baseline. Lower COPsub and higher thermal energy losses have a direct impact on the energy consumed to run the 5GDHC substation. In fact, there is an increase of the consumptions of electricity and thermal energy from the 5GDHC grid between 3.2÷4.2%.

It is also important to highlight how the MPC operation contributes to the electricity peak-load shaving by comparing the electricity consumption of the substation for the different scenarios during the off-peak and peak hours defined according to the TOU demand response strategy. It can be noticed that, in scenario 1 where a TOU price variation is not implemented, the effect of the MPC is to reduce the electricity consumption during the peak hours by 2.1% and to increase the one during the off-peak hours by 7.7%. Because a peak DHW load occurs in the morning between 7:00 and 9:00, the prediction of the MPC leads to the production of DHW

before the peak load occurs. When the TOU price variation is implemented in scenarios 2 and 3, this shift is further boosted. The higher the price variation, the higher is the amount of electricity consumption that is shifted to off-peak hours.

The economic performance of the different scenarios is summarised in Table 3. For the different cases, the total costs of the electrical (CEel,tot) and thermal energy (CEth,tot) consumption over the simulated period are calculated for the baseline scenario with the corresponding energy tariffs. For scenario 1 with a flat electricity price, the extra-charging processes with a peak temperature above 50°C due to the MPC outputs lead to higher electrical and thermal energy consumption with a total utility energy bill (UEBtot) that is higher than the baseline one by 3.7%. With the introduction of a TOU electricity tariff in scenario 2, the 5GDHC substation operation due to the MPC implicates a shift in the costs with a small reduction of the electricity bill and an increment of 3.2% of the thermal energy bill. Nevertheless, the relative difference in UEBtot is less than 1%. This means that a TOU energy tariff of that kind is still not effective for a final user that would like to install a predictive controller as already presented in a previous study [20]. This because the saving obtained by the limited price variation between off-peak and peak hours that occurs only two times a day during working days, does not compensate for the additional energy consumptions due to the drop in the 5GDHC substation performance and additional thermal losses of the TES. Finally, in scenario 2 it can be noticed that the situation is changed. The peak hours electricity tariff is four times that of off-peak hours. Here, the electricity bill savings achieved is about 6% whereas the thermal energy bill increases by 4.1% with respect to the baseline. The UEBtot has a reduction of 3.5% with respect to the baseline that makes the MPC system attractive with respect to a standard RBC system.

Table 2 Energy assessment of the parametric simulations.

| Scenario | $c_{el,off\text{-}peak}$ [EUR/kWh] | $c_{el,peak}$ [EUR/kWh] | $T_{top,max}$ [°C] | $T_{top,min}$ [°C] | $T_{ave}$ [°C] | $E_{el,sub}$ [kWh] | $E_{th,sub}$ [kWh] | $E_{th,load}$ [kWh] | $COP_{sub}$ [-] | $N_{on}$ [-] | $E_{el,sub,off\text{-}peak}$ [kWh] | $E_{el,sub,peak}$ [kWh] | $t_{disc}$ [%] |
|---|---|---|---|---|---|---|---|---|---|---|---|---|---|
| Baseline | | | 50.4 | 41.7 | 40.7 | 439.6 | 993.1 | 1224.0 | 2.78 | 101 | 258 | 182 | 2.1% |
| 1 | 0.15 | 0.15 | 54.1 | 43.7 | 41.2 | 455.8 | 1029.1 | 1226.1 | 2.69 | 172 | 278 | 178 | 1.6% |
| | | | *7.5%* | *4.7%* | *1.4%* | *3.7%* | *3.6%* | *0.2%* | *-3.4%* | *70.3%* | *7.7%* | *-2.1%* | *-24.7%* |
| 2 | 0.15 | 0.3 | 54.3 | 42.0 | 41.3 | 454.3 | 1025.2 | 1227.0 | 2.70 | 159 | 290 | 165 | 1.6% |
| | | | *7.7%* | *0.6%* | *1.5%* | *3.3%* | *3.2%* | *0.2%* | *-3.0%* | *57.4%* | *12.4%* | *-9.5%* | *-26.9%* |
| 3 | 0.15 | 0.6 | 54.3 | 43.5 | 41.4 | 458.2 | 1033.6 | 1228.3 | 2.68 | 169 | 302 | 156 | 1.5% |
| | | | *7.8%* | *4.3%* | *1.9%* | *4.2%* | *4.1%* | *0.3%* | *-3.7%* | *67.3%* | *17.3%* | *-14.2%* | *-32.2%* |

Table 3 Economic assessment of the parametric simulations.

| | $c_{El,off\text{-}peak}$ [EUR/kWh] | $c_{El,peak}$ [EUR/kWh] | $c_{Eth,dhc}$ [EUR/kWh] | $C_{El,tot}$ [EUR] | $C_{Eth,tot}$ [EUR] | $UEB_{tot}$ [EUR] |
|---|---|---|---|---|---|---|
| Baseline | 0.15 | 0.15 | 0.05 | 65.9 | 49.7 | 115.6 |
| Scenario 1 | 0.15 | 0.15 | 0.05 | 68.4 | 51.5 | 119.8 |
| Rel. var. | | | | *3.7%* | *3.6%* | *3.7%* |
| Baseline | 0.15 | 0.3 | 0.05 | 93.2 | 49.7 | 142.9 |
| Scenario 2 | 0.15 | 0.3 | 0.05 | 92.8 | 51.3 | 144.1 |
| Rel. var. | | | | *-0.4%* | *3.2%* | *0.8%* |
| Baseline | 0.15 | 0.6 | 0.05 | 147.9 | 49.7 | 197.5 |
| Scenario 3 | 0.15 | 0.6 | 0.05 | 139.0 | 51.7 | 190.7 |
| Rel. var. | | | | *-6.0%* | *4.1%* | *-3.5%* |

## 4. Conclusions

This work presents the implementation of an MPC controller that has been developed to optimise the operation of a 5GDHC substation to cover the DHW load by exploiting the thermal capacity of the DHW thermal

energy storage system. The controller structure is based on artificial neural networks (ANN) that have been used in a modular approach to create a surrogate model of the 5GDHC substation and the binary particle swarm optimization (BPSO) algorithm has been used in the optimizer to find the best trajectory over the prediction horizon according to the boundary conditions. The investigation reported in this study deals with two preliminary tests of the MPC controller. The results of test 1 highlight that using the same ANN model of the system as an emulator of the system can be useful in the debugging phase of the controller. Nevertheless, the results of the simulation are not representative for an accurate assessment of the system performance since the use of NARX ANN models involves the propagation of the errors of the outputs onto the input at each simulation timestep. To overcome these drawbacks, a platform that includes a co-simulation TRNSYS-LabVIEW has been developed. It includes a physical model of the system as an emulator and allows a reliable and accurate assessment of the MPC operation and system performance under close-to-reality boundary conditions.

The results of the second test presented in this study deal with the energetic and economic performance assessment of the 5GDHC substation comparing the system operation under a model predictive control (MPC) strategy compared to a standard rule based controller. Different scenarios have been analysed considering different electricity prices. In particular, a comparison between a flat electricity tariff with respect to time-of-use tariff is performed considering two different peak prices. The results show that the extra-charging process of the TES leads to a drop in system performance due to lower COP and higher thermal energy losses. This results in additional energy consumption of electricity and thermal energy that are not always compensated economically by the savings achieved by charging in a smart way the TES during the off-peak hours. In the best scenario, total bill savings of 3.5% have been achieved thanks to the MPC controller. Nevertheless, it is important to highlight how the MPC operation contributes to shaving the electricity peak-load providing flexibility to the power grid. For the two TOU scenarios, part of the electricity consumption is shifted to the off-peak period achieving a reduction of 9.5% and 14.2% in the peak-hours period with respect to the baseline. Further research is needed to extend the analysis to annual simulations and considering the MPC operation under real-time pricing (RTP) programs.

**Acknowledgements**

This work is part of the research activities of the project REWARDHeat funded by the European Union's Horizon 2020 research and innovation programme under grant agreement No 857811.

**References**

[1] S. Buffa, M. Cozzini, M. D'Antoni, M. Baratieri, and R. Fedrizzi, "5th generation district heating and cooling systems: A review of existing cases in Europe," *Renew. Sustain. Energy Rev.*, vol. 104, pp. 504–522, 2019.
[2] "Interreg project D2Grids." [Online]. Available: http://www.nweurope.eu/projects/project-search/d2grids-increasing-the-share-of-renewable-energy-by-accelerating-the-roll-out-of-demand-driven-smart-grids-delivering-low-temperature-heating-and-cooling-to-nwe-cities/.
[3] "REWARDHeat H2020 project." [Online]. Available: https://cordis.europa.eu/project/rcn/224317/fact-sheet/en. [Accessed: 13-Nov-2019].
[4] A. Afram and F. Janabi-Sharifi, "Theory and applications of HVAC control systems – A review of model predictive control (MPC)," *Build. Environ.*, vol. 72, pp. 343–355, Feb. 2014.
[5] A. Afram and F. Janabi-Sharifi, "Black-box modeling of residential HVAC system and comparison of gray-box and black-box modeling methods," *Energy Build.*, vol. 94, pp. 121–149, 2015.
[6] H. Esen, M. Inalli, A. Sengur, and M. Esen, "Predicting performance of a ground-source heat pump system using fuzzy weighted pre-processing-based ANFIS," *Build. Environ.*, vol. 43, no. 12, pp. 2178–2187, Dec. 2008.
[7] H. Esen and M. Inalli, "ANN and ANFIS models for performance evaluation of a vertical ground source heat pump system," *Expert Syst. Appl.*, vol. 37, no. 12, pp. 8134–8147, 2010.
[8] K. Li, H. Su, and J. Chu, "Forecasting building energy consumption using neural networks and hybrid neuro-fuzzy system: A comparative study," *Energy Build.*, vol. 43, no. 10, pp. 2893–2899, 2011.
[9] M. Lawrynczuk, *Computationally efficient model predictive control algorithms: a neural network approach*. New York: Springer, 2013.
[10] A. Afram, F. Janabi-Sharifi, A. S. Fung, and K. Raahemifar, "Artificial neural network (ANN) based model predictive control (MPC) and optimization of HVAC systems: A state of the art review and case study of a residential HVAC system," *Energy Build.*, vol. 141, pp. 96–113, Apr. 2017.

[11] M. L. Derouiche, S. Bouallègue, J. Haggège, and G. Sandou, "LabVIEW Perturbed Particle Swarm Optimization Based Approach for Model Predictive Control Tuning," *IFAC-Pap.*, vol. 49, no. 5, pp. 353–358, 2016.
[12] X. Zhao, "A perturbed particle swarm algorithm for numerical optimization," *Appl. Soft Comput. Elsevier*, vol. 10, pp. 119–124, 2010.
[13] "Advanced Metaheuristics Algorithms by ENIT." [Online]. Available: http://sine.ni.com/nips/cds/view/p/lang/it/nid/216789. [Accessed: 25-Oct-2018].
[14] Kennedy J. and Eberhart R.C., "A discrete binary version of the particle swarm algorithm," presented at the IEEE International Conference on Systems, Man, and Cybernetics. Computational Cybernetics and Simulation, Orlando, FL, USA, 1997.
[15] University of Wisconsin--Madison. Solar Energy Laboratory, *TRNSYS, a Transient Simulation Program.* Madison, Wis. :The Laboratory, 1975.
[16] R. Fedrizzi *et al.*, "FP7 INSPIRE project D6.3c: Performance of the Studied Systemic Renovation Packages – Multifamily Houses." 2015.
[17] U. Jordan and K. Vajen, "DHWcalc: Program to generate domestic hot water profiles with statistical means for user defined conditions," in *ISES Solar World Congress*, 2005, pp. 1–6.
[18] Eurac Research, "Energy Exchange Lab." [Online]. Available: http://www.eurac.edu/en/research/technologies/renewableenergy/Infrastructure/Pages/Energy-Exchange-Lab.aspx. [Accessed: 15-Dec-2017].
[19] R. Curtis and T. Pine, "Effects of cycling on domestic GSHPs. Supporting analysis to EA Technology Simulation / Modelling.," Mimer Geoenergy, Cornwall, 2012.
[20] Buffa S., Cozzini M., Henze G.P., Dipasquale C., Baratieri M., and Fedrizzi R., "Potential study on demand side management in district heating and cooling networks with decentralised heat pumps," presented at the International Sustainable Energy Conference - ISEC 2018, Graz, Austria.